

## **CIND Pre-Processing Pipeline For Diffusion Tensor Imaging**

### **Overview**

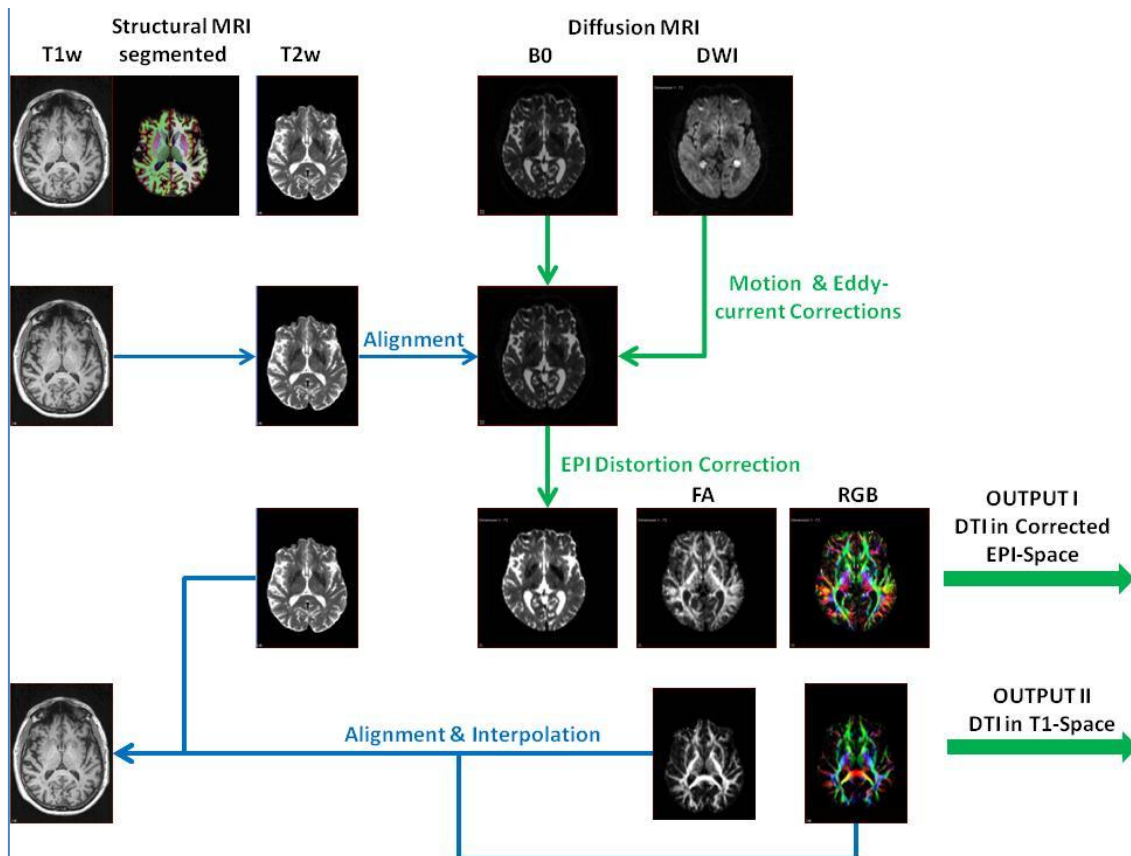
The preprocessing pipeline of the Center for Imaging of Neurodegenerative Diseases (CIND) prepares diffusion weighted images (DWI) and computes voxelwise diffusion tensors for the analysis of diffusion tensor imaging (DTI) data. Specifically the pipeline computes maps of diffusion eigenvalues and eigenvectors while also establishing an anatomical correspondence between DTI and structural MRI. For the computation of diffusion tensors, the pipeline uses TEEM tools (<http://teem.sourceforge.net/index.html>), a coordinated group of libraries for representing, processing, and visualizing scientific data developed by Gordon Kindlmann, University of Chicago). Prior to the tensor estimations, the pipeline performs corrections for distortions due to eddy currents and head motion. For the alignment between DTI and structural MRI, the pipeline further incorporates affine image registrations based on cost function weighting using FLIRT (<http://www.fmrib.ox.ac.uk/fsl/flirt/overview.html>) and nonlinear distortion corrections of DTI based on a variational matching algorithm described by Tao et al. <sup>(1)</sup>.

The output of the pipeline includes maps of diffusion summary measures, such as fractional anisotropy (FA) and mean diffusivity (MD) as well as eigenvectors and fiber directions. These DTI feature maps are provided in two representations. In the first presentation, the DTI feature maps are provided in the corrected echo-planar imaging (EPI) space in which geometrical discrepancies between DTI and structural MRI are reduced. In the second representation, the DTI feature maps in the corrected EPI-space are mapped into the space of the T1-weighted structural MRI data and resolution is interpolated to that of the structural MRI for better anatomical visualization. Each representation provides users with a variety of options to perform subject-specific and group-specific analysis of DTI data, such as statistical parametric mapping and tractography.

## Main Processing Steps of the Pipeline

The processing pipeline involves several major steps, as illustrated in the flow chart and described in more detail further below.

Processing Flow Chart



1. In the first step, the diffusion weighted images (DWI) are imported in the pipeline and each frame is corrected for eddy current distortions and head motion. Eddy current correction describes the correction of geometrical shifts and intensity variations due to a transient magnetic field induced by eddy-currents. Transformation and intensity corrections from eddy-current distortions are computed following the procedures outlined by Rohde et al. <sup>(2)</sup>. Head motion correction is accomplished by modeling displacement and changes in orientation of a brain image as a rigid body transformation (affine) with nine degrees of freedom to correct for rotations, translations and scaling.
2. Next, preprocessed structural T1-weighted and density/T2-weighted MRI data are affine aligned with the b0 map image of DWI based on mutual information metric. The T1-weighted MRIs are further processed with Freesurfer (<http://surfer.nmr.mgh.harvard.edu/>) to automatically generate a skull-stripping mask, which is then applied to the co-registered T2-

weighted MRIs in T1 image space. The b0 map is also preprocessed for skull-stripping prior to the T2/b0 alignment.

3. A deformation field is then calculated to accomplish an anatomical correspondence between DWI and structural MRI frames using variational matching as proposed by Tao et al. <sup>(1)</sup>. The deformation field accounts for geometrical discrepancies between DWI and structural MRI due to static magnetic susceptibility variations which distort DWI (since the acquisition is based on echo-planar imaging, EPI). The strategy used here is to nonlinearly warp the b0 image of the DWI acquisition with the corresponding T2-weighted structural image, co-registered and interpolated into the native b0 image space. To reduce the distortions, the variational matching method exploits simultaneously the high correlation between the b0 image and T2-weighted image and the conservation of the signal between the uncorrected and corrected DWI data. The deformation field and eddy-current transformations are then concatenated and applied to the DWI images, yielding corrected EPI representations of DWI.
4. For the corrected EPI representation of DTI, the diffusion tensors are calculated voxel-by-voxel and maps of the eigenvalues and eigenvectors are reported. For the tensor estimation, a nonlinear fitting library of TEEM is used that relates variations of the DWI signal to the diffusion sensitization gradients with the b0 image(s) as normalization factor. Specifically, the ‘tend estim’ tool in TEEM is used for a weighted-least-squares fitting of DWIs to estimate the diffusion tensors in the corrected EPI-space with the b0 reference image <sup>(3)</sup>. B-matrix characterizing the diffusion weighting for each image is learned from the input image. In addition, ‘tend estim’ automatically estimates a thresholding value, which is determined by a soft-thresholding of an Otsu classification of all the DWI values <sup>(4)</sup>. This has the effect of masking out background and low signal intensity voxels. The way diffusion tensors are represented in the NRRD format is with 7 values: a mask or confidence value, and then the 6 unique diffusion tensor components. The maps of eigenvalues and eigenvectors are generated from the estimated DTI. The three eigenvalues are ranked in magnitude from the largest (L1) to the smallest (L3).
5. For the T1-space representation of DTI the following strategy is applied: First the T2-weighted structural MRI is registered to the T1-weighted structural MRI by an affine transformation with 6 degrees of freedom, using again FLIRT (<http://www.fmrib.ox.ac.uk/fsl/flirt/overview.html>). The same transformation is then applied to the b0 image(s) and DWI data as well as to the coordinates of the diffusion sensitization gradients thereby accomplishing a complete representation of DWI in the T1-space. Resolution of DWI is boosted to match that of the T1-weighted structural MRI using trilinear interpolation. The diffusion tensors are calculated according to point #4 above and the maps of the eigenvalues and eigenvectors are generated.
6. For some applications, several DTI summary measures are provided, including several indices of fractional anisotropy. For the definition of the summary measures see also reference (5). Let the diffusion tensor be  $\mathbf{D}$  with the three eigenvalues  $\lambda_i, i = 1, 2, 3$ . Then:
  - a. *Mean Diffusivity:*

$$MD = \frac{1}{3} \text{tr} \mathbf{D} = \frac{1}{3} \sum_{i=1}^3 \lambda_i$$

b. Conventional fractional anisotropy (Euclidian distance):

$$FA = \frac{A_{euc}}{\sqrt{\text{tr}(\mathbf{D}\mathbf{D}^T)}}, \text{ with: } A_{euc} = \sqrt{\text{tr}\mathbf{D}^2 - 1/3 \cdot \text{tr}^2\mathbf{D}} = \sqrt{\frac{2}{3}} \cdot \sqrt{\sum_i \lambda_i^2 - \sum_{1 \leq i < j \leq n} \lambda_i \lambda_j}$$

Note, this formula of FA is more concisely written but otherwise equivalent to the more familiar expression of FA as coefficient of variation.

c. Geodesic fractional anisotropy (Riemann distance):

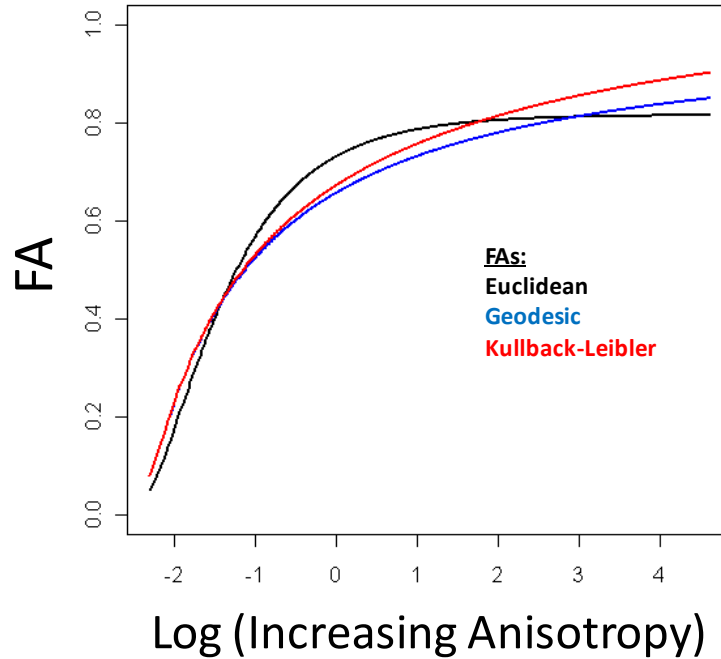
$$GA = \frac{A_{geo}}{1 + A_{geo}}, \text{ with: } A_{geo} = \sqrt{\text{tr} \ln^2 \mathbf{D} - 1/3 \cdot \text{tr}^2 \ln \mathbf{D}} = \sqrt{\frac{2}{3}} \cdot \sqrt{\sum_i \ln \lambda_i^2 - \sum_{1 \leq i < j \leq n} \ln \lambda_i \cdot \ln \lambda_j}$$

d. Symmetrized Kullback-Leibler fractional anisotropy:

$$KLA = \frac{A_{kl}}{1 + A_{kl}}, \text{ with: } A_{kl} = \sqrt{2\sqrt{\text{tr}\mathbf{D} \cdot \text{tr}\mathbf{D}^{-1}} - 3} = \sqrt{2\sqrt{\sum_i \lambda_i \cdot \sum_i \lambda_i^{-1}} - 2 \cdot 3}$$

The change of each FA index as a function of increasing tensor anisotropy is illustrated in the figure below. Note, the increasing anisotropy on the horizontal axis is plotted on a logarithmic scale. The three FA indices are similar for closely isotropy tensors but as anisotropy increases, GA and KLA change quite differently from the Euclidean FA. Specifically, GA and KLA increase more monotonically than the Euclidean FA. Experimentally, both GA and KLA may have an advantage over Euclidean FA for diffusion data with high anisotropy but on the other hand GA and KLA are more susceptibility to noise but this still needs to be explored in more detail.

## Changes of Various FA Indices



## Outputs

The following maps are provided:

### In corrected EPI space

- |                          |   |
|--------------------------|---|
| 1. EigenVal1-EPI.nii     | -> largest eigenvalue                             |
| 2. EigenVal2-EPI.nii     | -> middle eigenvalue                              |
| 3. EigenVal3-EPI.nii     | -> smallest eigenvalue                            |
| 4. EigenVectors-EPI.nrrd | -> eigenvectors                                   |
| 5. RGB-EPI.nhdr          | -> fiber directions as red/green/blue model (RGB) |
| 6. FA-EPI.nii            | -> standard fractional anisotropy (Euclidian)     |
| 7. MD-EPI.nii            | -> standard fractional anisotropy                 |

### In T1-space

- |                      |                        |
|----------------------|------------------------|
| 1. EigenVal1-MRI.nii | -> largest eigenvalue  |
| 2. EigenVal2-MRI.nii | -> middle eigenvalue   |
| 3. EigenVal3-MRI.nii | -> smallest eigenvalue |

- |                          |  |
|--------------------------|--|
| 4. EigenVectors-MRI.nrrd | -> eigenvectors  |
| 5. RGB-MRI.nrrd          | -> fiber directions as RGB model (red: right-left, green:anterior-posterior, blue:inferior-superior) |
| 6. FA-EPI.nii            | -> standard fractional anisotropy (Euclidian)  |
| 7. GA-EPI.nii            | -> geodesic fractional anisotropy (non-Euclidian)  |
| 8. KLA-EPI.nii           | -> Kullback-Leibler fractional anisotropy (non-Euclidian)  |

## Limitations

The current implementation of the DTI pipeline has several limitations:

- 1) Eddy-current corrections: This procedure is limited to effects from eddy-currents that have negligible decays during the DTI readout and either reach state-state or die away between consecutive slice excitations. Effects from eddy currents with shorter decays are not corrected and result in image blurring. Furthermore, eddy-currents that do not die away between consecutive slices induce distortions in the first few DTI frames until the eddy-currents reach steady-state.
- 2) Deformation field: The method of variational matching for the distortion correction in DWI does not account for intensity variations due to pixel aliasing. Thus, DWI values from regions with prominent susceptibility distortions should be interpreted with caution. Furthermore, the nonlinear deformations may alter the topology in DTI, complicating tractography.
- 3) Tensor computation: The semi-positive characteristic of the diffusion tensor is not strictly enforced for the tensor computation. Hence, negative eigenvalues (which are physically meaningless) can occur to the extent of measurement errors.

## References

- (1) Ran Tao, P. Thomas Fletcher, et al. (2009). "A Variational Image-Based Approach to the Correction of Susceptibility Artifacts in the Alignment of Diffusion Weighted and Structural MRI." *Process Med Imaging* 21: 664-675.
- (2) G.K. Rohde, A.S. Barnett, P.J. Basser, S. Marengo, and C. Pierpaoli. Comprehensive Approach for Correction of Motion and Distortion in Diffusion-Weighted MRI. *Magnetic Resonance in Medicine* 51:103–114 (2004).
- (3) R. Salvador, A. Pena, D. K. Menon, T. A. Carpenter, J. D. Pickard, and E. T. Bullmore. Formal characterization and extension of the linearized diffusion tensor model. *Hum Brain Mapp*, 24(2):144–55, 2005.
- (4) Nobuyuki Otsu (1979). "A threshold selection method from gray-level histograms". *IEEE Trans. Sys., Man., Cyber.* 9 (1): 62–66.
- (5) M. Moakher and PG Batchelor. Symmetric Positive Definite Matrices: From Geometry to Applications and Visualization. In: *Visualization and Processing of Tensor Fields*. Eds: Weickert and Hagen. Springer, Heidelberg (2006).